AN EXPERIMENTAL DISCUSSION ON EFFECT OF MAXIMUM AGGREGATE SIZE PARAMETERS OF SFRC ON MODE-1

CHODAVARAPU GIRIDHAR KUMAR[1]
Assistant Professor, Department of Civil Engineering,
JNTU GV – CEV, Vizianagaram, India.
giridharkumarch.ce@gmail.com

RAMBA BALA MURALI KRISHNA[2]
Assistant Professor, Department of Civil Engineering,
JNTU GV – CEV, Vizianagaram, India.
balupvp@gmail.com

T S D PHANINDRANATH[3]
Assistant Professor, Department of Civil Engineering,
JNTU GV – CEV, Vizianagaram, India.
Phani.civil485@gmail.com

VANKADARA SAMPATH KUMAR[4]
Department of Electrical and Electronics Engineering,
Malla Reddy Engineering College(Autonomous),Maisammaguda
Hyderabad, India.
sampath.vankadara62@gmail.com

ADDEPALLI VENKATA SURYA GOWTHAM[5]
Assistant Professor, Department of Mechanical Engineering,
JNTU GV – CEV, Vizianagaram, India.
gowthamaddepalli@gmail.com

P MALLIKARJUN[6]
Department of Electrical and Electronics Engineering
Malla Reddy Engineering College(Autonomous),Maisammaguda,
Hyderabad, India.
pernemallikarjun@gmail.com

***Abstract*— Improved forecasts about the lifespan and robustness of a structure in the event of fractures are possible thanks to the theories of fracture mechanics. Moderate A fracture mechanics approach using the Size Effect Law is used to simulate the propagation of cracks in steel fiber-reinforced concrete (SFRC). In this current experimental study, geometrically comparable notched prismatic specimens composed of fibre concrete containing 0.5%, 1%, and 1.5% of steel fibres were tested against plain concrete. The study used three different MAS: 20mm, 16mm, and 10mm. Three point bending testing is used to evaluate the notched specimens. In addition to other parameters of concrete like Young's modulus (E), cohesive fracture zone (Cf), failure stress (σn), and brittleness number (β), theories of fracture mechanics typically include the fracture energy (Gf) of concrete as a significant feature. It is possible to derive the fracture energy parameters from the curves of P-δ, P-CMOD, β-d, and σn-d. In order to calculate fracture toughness, several relationships are constructed by altering the fraction of steel fibres and the Maximum Aggregate Size versus load. Concrete's post peak behaviour can be ascertained by utilising the area under the p-δ curves.**

Keywords— **Fracture, Steel fibres, concrete, post-peak behaviour.**

I. INTRODUCTION

Concrete crack formation poses a serious risk of damage due to corrosion, necessitating accurate prediction for mitigation. The fictitious crack model (FCM), pioneered by Hillerborg in 1976, emerges as a potent tool for anticipating cracks in composite materials like concrete. Realistic predictions hinge on understanding fracture energy and material strain softening. Strength, alongside parameters like ductility, self-compacting ability, and wear resistance, plays a crucial role. The focus of this talk is on crack development in regular concrete, where the mechanical interactions between the cement-based matrix and aggregates determine the fracture energy and strain softening dynamics, which are closely related to the composite structure. There are many different reasons why things fail, such as unknown loading, flaws in the materials, inadequate design, and poor construction. Designing against fractures constitutes a dynamic research area crucial for structural engineers. Emphasizing the vulnerability of increasingly brittle materials, especially when life is at stake, underscores the need for meticulous consideration of numerous failure-contributing factors. Engineers must be well-versed in available procedures to safeguard against catastrophic, brittle fractures, a significant contributor to engineering disasters.

The literature distinguishes between the three different fracture modes shown in figure.

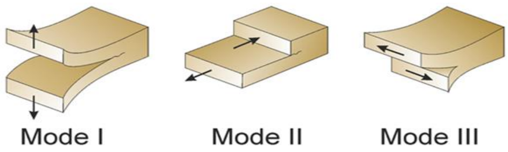

Fig. 1. Different fracture modes

Mode I: OPENING MODE OR TENSILE MODE
Mode II: SLIDING MODE OR IN-PLANE SHEAR MODE
Mode III: TEARING MODE OR ANTI PLANE SHEAR MODE

II. EXPERIMENTAL PROGRAMME:

A. *Methodology of Experimentation:*

The purpose of the experimental programme was to determine the fracture energy and stress intensity factor of Steel Fibre Reinforced Concrete (SFRC) beams with a centrally placed notch at mid-span under a three-point bending test, or with a central point load. The beams had dimensions of 100 mm x 75 mm x 350 mm (Span is 300 mm), 100 mm x 150 mm x 650 mm (Span is 600 mm), and 100 mm x 300 x 1250 mm (Span is 1200 mm). The impact of specimens with a notch positioned in the centre on stress intensity and fracture energy was examined using beams with two distinct mix proportions and various sizes. (M20 and M30) with varying percentage of steel fibres (0.5%,1%,1.5%) and Maximum Aggregate Size (MSA) taken as (20mm,16mm,10mm).

For every grade in this experimental programme, there are three series of beams with similar notch depth ratios (0.15): small, medium, and large.

The beams were designated in order of grade and were given alphabets for naming of grade. (M20-A, M30- B).The aggregate size is given in numbers followed by size of aggregate. (20mm-1,16mm-2,10mm-3). The beam size is given as (small-S, medium-M, large-L). The percentage of steel fibres were written at the end as (0%,0.5%,1%.1.5%).
The beams were named as **(A, B) x / (S, M, L) / y%**
Here A, B are grade of concrete viz. A-M20 & B-M30
X is 1,2,3. i.e., 1-20mm,2-16mm,3-10mm.
Size of beams were given as S-small, M-medium, L-large.
Y represents percentage of steel fibers viz. 0%,0.5%,1%,1.5%.
Finally beams were designated as
M20(A),20mm (1), large beam(L),0%--[**A1/L/0%**]
M30(B).20mm (1). large beam(L).0%--[**B1/L/0%**]

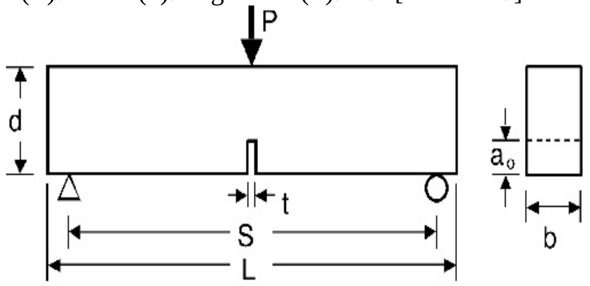

Fig. 2. The Three point bending Test Setup

Where

P = LOAD APPLIED ON BEAM
d = DEPTH OF THE BEAM
S = SPAN OF BEAM
L = TOTAL LENGTH OF BEAM
a_0 = CRACK WIDTH

B. Materials:-

Moulds preparation: Common cast iron cylinders and cubes serve as moulds. Cubes and cylinders were cast using moulds. For the purpose of casting beams in the following sizes (l*h*b), three cast iron moulds were prepared.

1. 350*75*100 mm
2. 650*150*100 mm
3. 1250*300*100 mm

Providing Notch: A marble cutter was used to cut the beams into the concrete that had set.

III. Results and Discussions:

A. Test Setup and Testing Procedure:

Every specimen was put through its paces of 0.02 mm per minute displacement control testing on a 100 TONNE capacity loading frame. The samples were removed from the curing tank and left to dry after 28 days of curing. Next, a notch with a notch to depth ratio of 0.15 is provided at the centre of the beam. Subsequently, white wash was applied to the sample. The material was retained for testing for a day. As seen in the figure below, the notched beam specimen was maintained on the testing machine's supports. When conducting a test, the notched beam is subjected to a progressively higher load until a stress threshold is reached that causes cracks to spread.

Fig. 2. Loading Frame Test Setup Used for Testing of Beams

B. Regression Graphs for M20&M30:

Regression graphs were plotted between Y (y-axis) and depth (x-axis) of beam from which the constants A and C are determined. These constants are used to determine Fracture Energy (Gf).

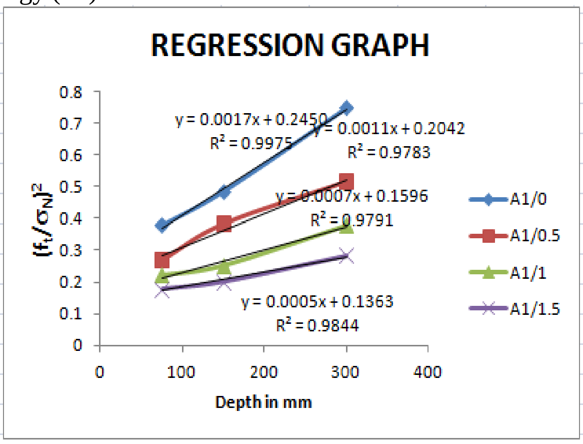

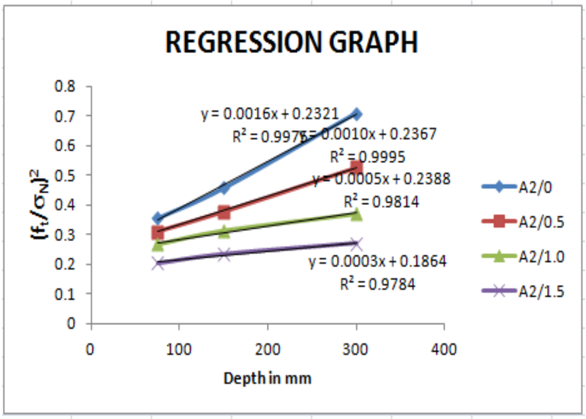

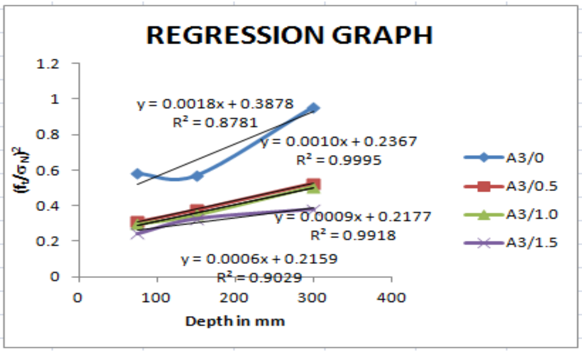

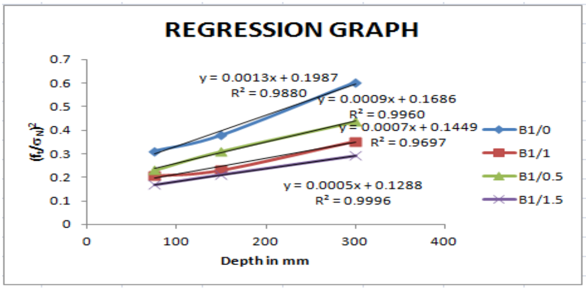

Brittleness number Vs Depth: Graphs were plotted between Brittleness number β (d/do) and depth (mm) from which the brittleness natures of specimens are determined. The graphs were plotted considering the percentage of steel fibres.

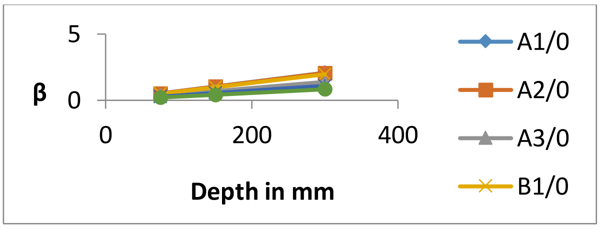

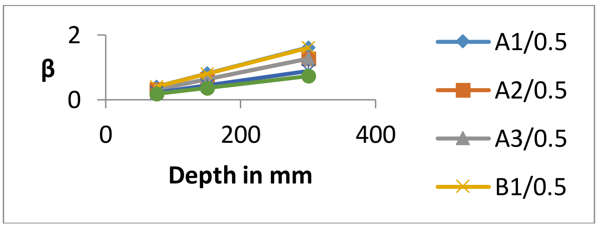

Failure Stress Vs Depth: Failure stress (σn) is determined and graphs are plotted between failurestress and depth(mm). Failure stress increases when MAS increases from 10 to 20 mm.

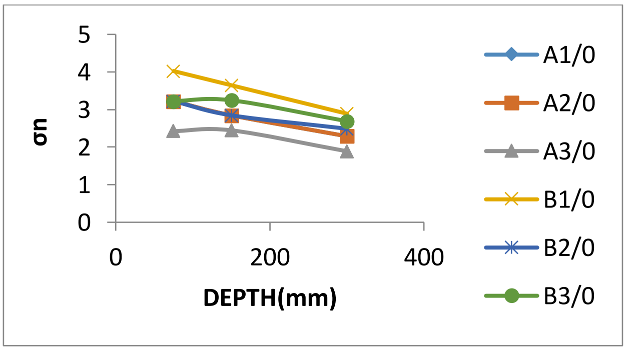

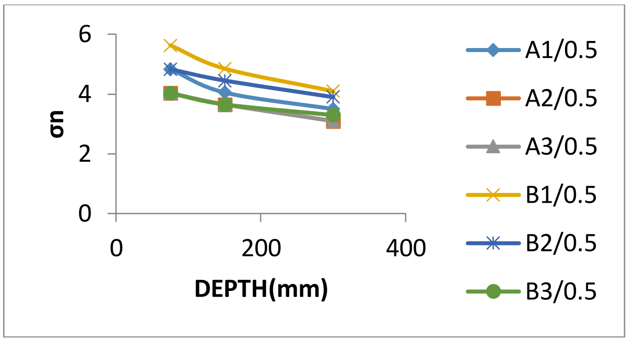

Load Vs Deflection: The load-bearing capability of the specimens improves as the proportion of steel fibres increases, as shown in this graph between load and deflection. This clearly indicates that the specimens' ductility is higher in large beams.

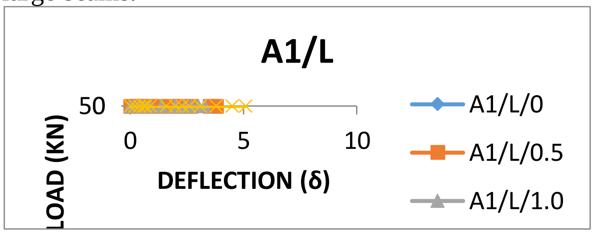

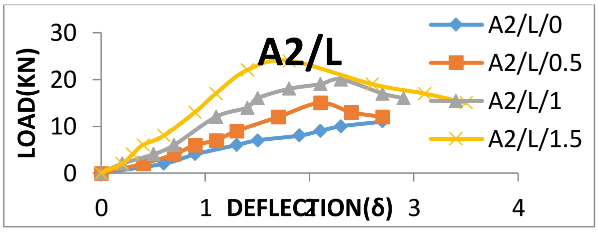

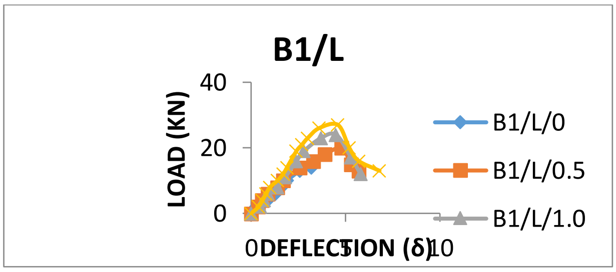

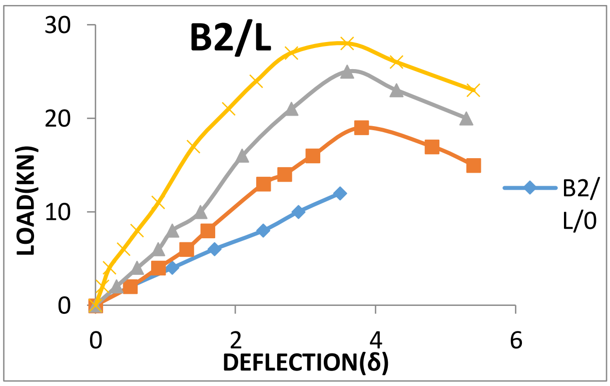

Fig. 3 .Load Vs CMOD

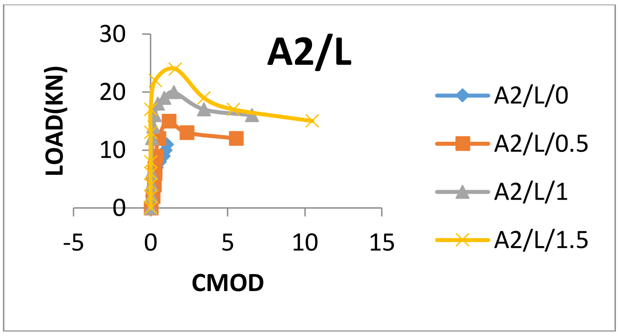

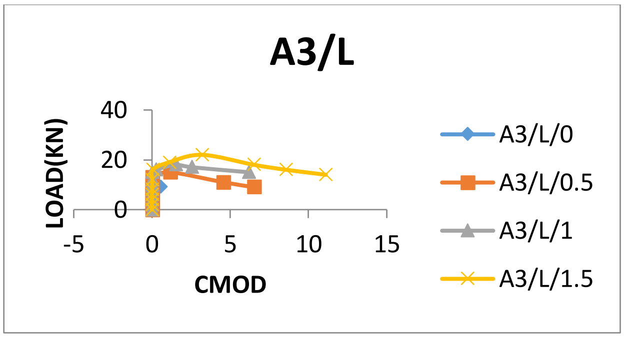

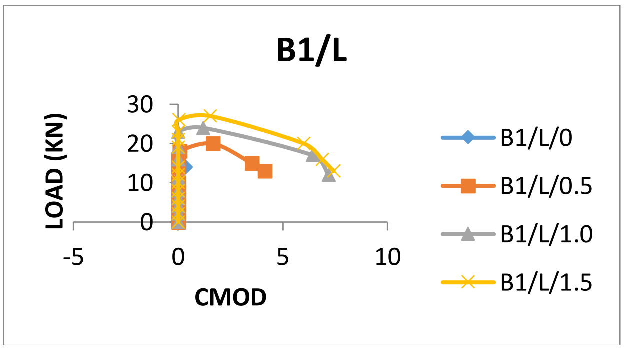

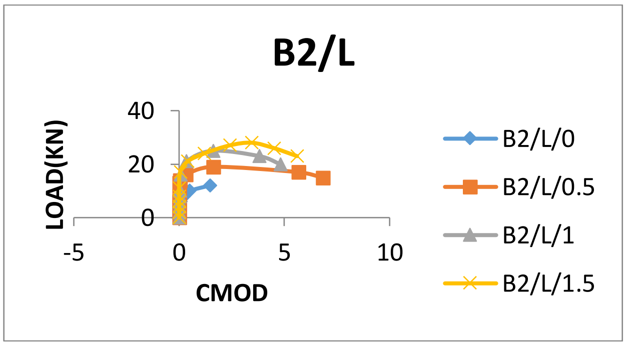

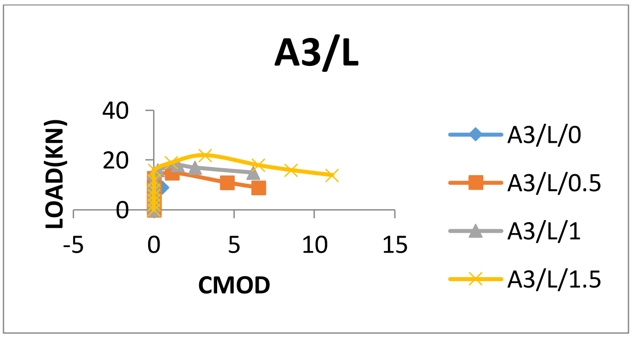

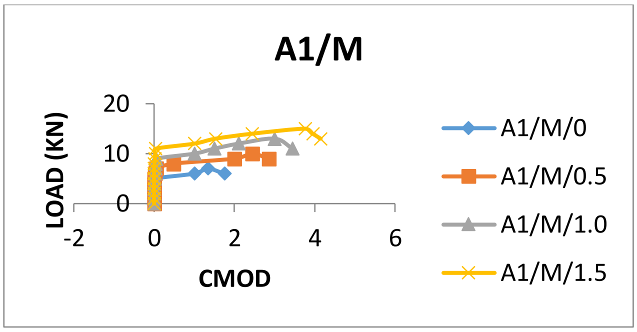

Calculated fracture energy (Gf) is shown against the proportion of steel fibres on graphs. Graphs can be used to study the behaviour of fracture energy as steel fibres increase in number.

Fracture Energy Vs Percentage of steel fibers:

Graphs are plotted between Fracture energy and percentage of steel fibers and the behavior of Gf is studied when there is increase in aggregate size.

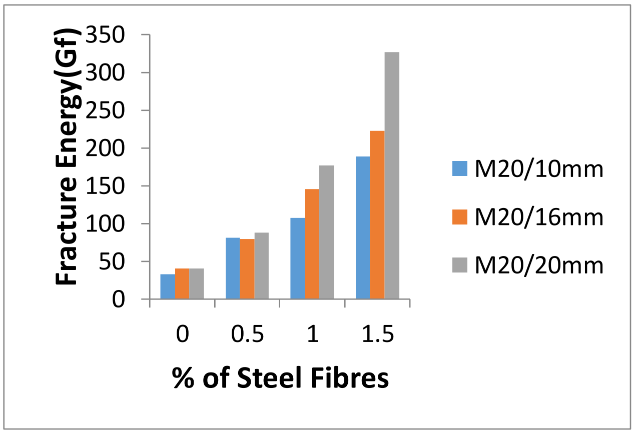

M20 Grade

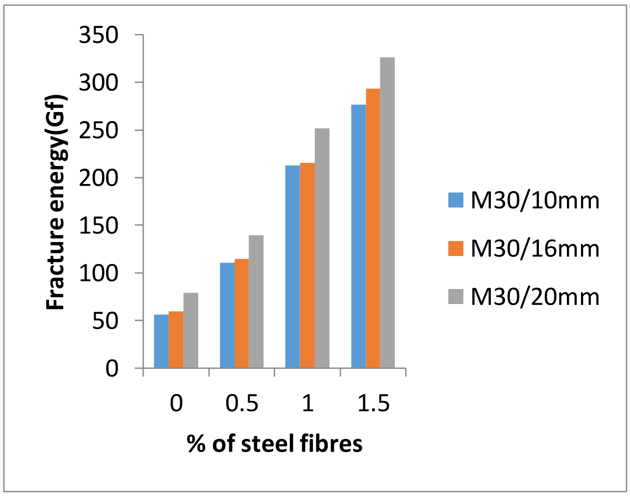

M30Grade

Fracture Energy Vs MAS: Graphs are plotted between Fracture energy and MAS and the behavior of Gf is studied when there is increase in aggregate size.

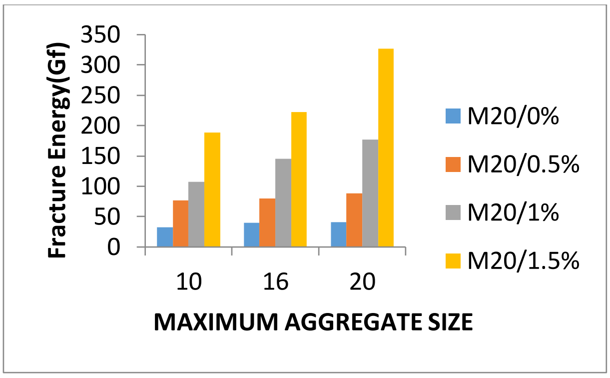

M20 Grade

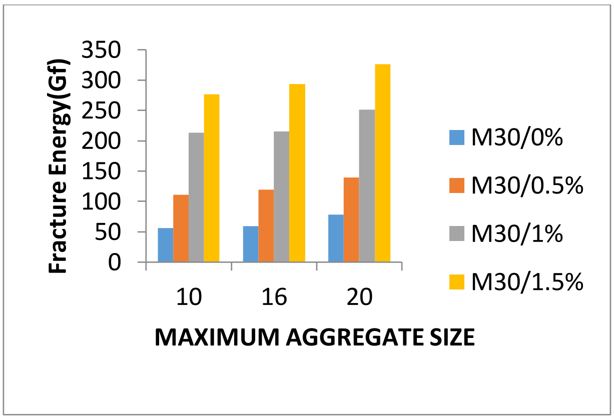

M30 Grade

Fig. 4. BEAMS BEFORE TEST (A)

Fig. 5. BEAMS AFTER TEST(A)

TABLE 1: DIMENSIONS OF BEAM SPECIMENS IN SIZE EFFECT METHOD

CONCRETE GRADE	SPECIMEN	SIZE OF AGGREGATE (mm)	Length(L) mm	Width(b) mm	Depth(d) mm	Span(S) mm	Depth of Notch(ao)	ao/d	S/d
M20	SMALL	10	350	100	75	300	11.25	0.15	4
		16	650	100	150	600	22.5	0.15	4
		20	1250	100	300	1200	45	0.15	4
M20	MEDIUM	10	350	100	75	300	11.25	0.15	4
		16	650	100	150	600	22.5	0.15	4
		20	1250	100	300	1200	45	0.15	4
M20	LARGE	10	350	100	75	300	11.25	0.15	4
		16	650	100	150	600	22.5	0.15	4
		20	1250	100	300	1200	45	0.15	4
M30	SMALL	10	350	100	75	300	11.25	0.15	4
		16	650	100	150	600	22.5	0.15	4
		20	1250	100	300	1200	45	0.15	4
M30	MEDUM	10	350	100	75	300	11.25	0.15	4
		16	650	100	150	600	22.5	0.15	4
		20	1250	100	300	1200	45	0.15	4
M30	LARGE	10	350	100	75	300	11.25	0.15	4
		16	650	100	150	600	22.5	0.15	4
		20	1250	100	300	1200	45	0.15	4

TABLE 2: QUANTITIES OF MATERIALS

GRADE	SIZE OF AGGREGATE (mm)	PROPORTIONS	CEMENT (Kg/m3)	WATER (Kg/m3	FINE AGGREGATE (Kg/m3)	COARSE AGGREGATE (Kg/m3)	STEEL FIBERS (Kg)
M20	10	0.5:1:1.46:2.54	277.96	138.98	405.821	706.01	28.376
	16	0.5:1:1.38:2.98	266.28	133.141	367.48	785.00	28.376
	20	0.5:1:1.425:3.1	258.40	129.20	368.22	801.04	28.376
M30	10	0.46:1:1.29:2.55	302.12	138.98	389.74	770.41	28.376
	16	0.46:1:1.28:2.88	289.44	133.20	370.50	833.60	28.376
	20	0.46:1:1.26:3.12	281.00	129.28	354.10	876.72	28.376

TABLE 3: (A)SPECIFICATIONS OF QUANTITIES OF MATERIALS

Specimen	Regression A	Regression C	Failure Stress(σN)	Brittleness Number(β)	Fracture Energy Gf(N/mm)	Cf	Ki
B1/S/0	0.0013	0.1987	4.0252	0.49068948	58.17797	17.57705	23.61646
B1/M/0	0.0013	0.1987	3.6468	0.98137896	58.17797	17.57705	30.25898
B1/L/0	0.0013	0.1987	2.89	1.96275793	58.17797	17.57705	33.91214
B1/S/0.5	0.0009	0.1686	5.62625	0.40035587	114.4855	21.54302	33.01007
B1/M/0.5	0.0009	0.1686	4.84875	0.80071174	114.4855	21.54302	40.23205
B1/L/0.5	0.0009	0.1686	4.09375	1.60142349	114.4855	21.54302	48.03731
B1/S/1	0.0007	0.1449	6.4021	0.36231884	151.8167	23.80466	37.5621
B1/M/1	0.0007	0.1449	6.04875	0.72463768	151.8167	23.80466	50.18894
B1/L/1	0.0007	0.1449	4.89375	1.44927536	151.8167	23.80466	57.42476
B1/S/1.5	0.0005	0.1288	7.22625	0.29114907	226.4293	29.62357	42.39751
B1/M/1.5	0.0005	0.1288	6.44875	0.58229814	226.4293	29.62357	53.5079
B1/L/1.5	0.0005	0.1288	5.49375	1.16459627	226.4293	29.62357	64.46534
B2/S/0	0.0015	0.4119	3.2252	0.27312455	56.05185	31.57854	18.92274
B2/M/0	0.0015	0.4119	2.8468	0.54624909	56.05185	31.57854	23.62106
B2/L/0	0.0015	0.4119	2.49	1.09249818	56.05185	31.57854	29.21842
B2/S/0.5	0.0008	0.2706	4.82625	0.22172949	139.7492	38.89819	28.31635
B2/M/0.5	0.0008	0.2706	4.44875	0.44345898	139.7492	38.89819	36.91309
B2/L/0.5	0.0008	0.2706	3.89375	0.88691796	139.7492	38.89819	45.69045

TABLE 3: (B)SPECIFICATIONS OF QUANTITIES OF MATERIALS

Specimen	Regression A	Regression C	Failure Stress(σN)	Brittleness Number(β)	Fracture Energy Gf(N/mm)	Cf	Ki
A1/S/0	0.0017	0.245	3.2252	0.520408163	40.57721	16.57329	18.92274
A1/M/0	0.0017	0.245	2.8468	1.040816327	40.57721	16.57329	23.62106
A1/L/0	0.0017	0.245	2.29	2.081632653	40.57721	16.57329	26.87156
A1/S/0.5	0.0011	0.2042	4.82625	0.404015671	88.32024	21.34787	28.31635
A1/M/0.5	0.0011	0.2042	4.04875	0.808031342	88.32024	21.34787	33.59413
A1/L/0.5	0.0011	0.2042	3.49375	1.616062684	88.32024	21.34787	40.99673
A1/S/1	0.0007	0.159	5.6021	0.330188679	145.4878	26.12105	32.86838
A1/M/1	0.0007	0.159	5.24875	0.660377358	145.4878	26.12105	43.55101
A1/L/1	0.0007	0.159	4.29375	1.320754717	145.4878	26.12105	50.38417
A1/S/1.5	0.0005	0.1363	6.42625	0.275128393	222.8431	31.34855	37.70379
A1/M/1.5	0.0005	0.1363	6.04875	0.550256787	222.8431	31.34855	50.18894
A1/L/1.5	0.0005	0.1363	5.09375	1.100513573	222.8431	31.34855	59.77162
A2/S/0	0.0016	0.2321	3.2252	0.517018526	40.12807	16.68195	18.92274
A2/M/0	0.0016	0.2321	2.8468	1.034037053	40.12807	16.68195	23.62106
A2/L/0	0.0016	0.2321	2.29	2.068074106	40.12807	16.68195	26.87156
A2/S/0.5	0.001	0.2367	4.02625	0.316856781	79.51799	27.22011	23.62262
A2/M/0.5	0.001	0.2367	3.64875	0.633713561	79.51799	27.22011	30.27516
A2/L/0.5	0.001	0.2367	3.09375	1.267427123	79.51799	27.22011	36.30301

The mix proportions were used to cast 6 beams (2S,2M,2L), 3 cubes and 3 cylinders per mix. Steel fibres are taken by volume fraction viz. 0%,0.5%,1%,1.5%.

IV. CONCLUSIONS

The following analysis of the test data was done using 144 specimens that were geometrically identical.

- The fracture energy (Gf) increases as the maximum aggregate size (MAS) and percentage of steel fibres increase.
- Failure stress rises by 80% for A series and 86% for B series with a MAS increase of 10mm to 20mm. Failure Stress (σn) rises by 47.5% in the A series and 55.08% in the B series with an increase in steel fibre percentage from 0% to 1.5%.
- Brittleness number increases by 33.4% in the B series and 66.9% in the A series with a 20mm MAS increase. with a rise in steel fibre content from 0% to 1.5% In the A series, the brittleness number drops by 52.76%, and in the B series, by 59.5.
- The Fracture Process Zone (FPZ), or Cf, drops by 64.89% in the A series and 42.31% in the B series when the MAS is increased from 10mm to 20mm. In the A series, FPZ(Cf) grows by 52.85%, and in the B series, by 59.32%, with an increase in the percentage of steel fibres from 0% to 1.5%.

- Increase in both MAS and steel fibre % lead to an improvement in the post peak behaviour (p-δ) of concrete.

References

[1] Z.P. Bazant, B.H. Oh, Crack band theory for fracture of concrete, Materials and Structures 16 (1983) 155–177.

[2] A. Hillerborg, M. Modeer, P.E. Petersson, Analysis of crack formation and crack growth in concrete by means of fracture mechanics and finite elements, Cement and Concrete Research 6 (6) (1976) 773–782.

[3] G. Cusatis, Z.P. Bazant, L. Cedolin, Confinement-shear latticemodel for concrete damage in tension and compression: I. theory, ASCE Journal of Engineering Mechanics 129 (12) (2003) 1439–1448.

[4] G. Cusatis, Z.P. Bazant, L. Cedolin, Confinement-shear lattice model for concrete damage in tension and compression: II. computation and validation, ASCE Journal of Engineering Mechanics 129 (12) (2003) 1449–1458.

[5] Z.P. Bazant, G. Pijaudier-Cabot, Nonlocal continuum damage localization instability and convergence, ASME Journal of Applied Mechanics 55 (1988) 287–293.

[6] J.P.B. Leite, V. Slowik, H. Mihashi, Computer simulation of fracture processes of concrete using mesolevel models of lattice structures, Cement and Concrete Research 34 (2004) 1025–1033.

[7] L. Cedolin, S.D. Poli, I. Iori, Experimental determination of the fracture process zone in concrete, Cement and Concrete Research 13 (1983) 557–567.

[8] Planas J, Guinea GV, Elices M. Size effect and inverse analysis in concrete fracture. Int J Fracture 1999;95:367–78.

[9] Heilmann HG, Hilsdorf H, Finsterwalder K. Festigkeit und verformung von beton unter zugspannungen. Deustcher Ausshuss fur Stahlbeton 1969:203.

[10] Cedolin L, Dei Poli S, Iori I. Tensile behavior of concrete. ASCE J Eng Mech 1987;113(3):431–49.

[11] Guinea GV, Planas J, Elices M. Measurement of the fracture energy using three point bend tests Part 1– Influence of experimental procedures. Mater Struct 1992;25:212–8. Carlucci A. Interaction between concrete fracture and bond (in Italian). Master Thesis, Politecnico di Milano University, 2003.

[12] Auriemma M, Avogadri M. Fracture properties of concrete (in Italian). Master Thesis, Politecnico di Milano University, 2005.

[13] Tada H, Paris PC, Irwin GR .The stress analysis of cracks handbook. Saint Louis (MO): Paris Productions; 1985.

[14] Taini, G. 2002. Experimental determination of fracture energy of concrete (Italian). Master Thesis, Politecnico di MilanoUniversity; 2002.

[15] Barcillesi A, Baroni S. Experimental determination of fracture characteristics of concrete (in Italian).Master Thesis, Politecnico di Milano University; 2003.

[16] Al-Shayea NA. Crack propagation trajectories for rocks under mixed modes I–II fracture. Engng Geol 2005;81:84–97.

[17] Weibull W. Phenomenon of rupture in solids. Ingenioersvetenskaps Akad Handl 1939;153:1–55.

[18] Leicester RH. The size effect of notches. In: Proceedings of the second Australasian conference on mechanics of materials and structures. Melbourne;1969. p. 1–20.

[19] Aliha MRM, Ayatollahi MR, Smith DJ, Pavier MJ. Geometry and size effects on fracture trajectory in a limestone rock under mixed mode loading. Engng Fract Mech 2010;77:2200–12.

[20] Bazant ZP. Crack band model for fracture of geomaterials. In: Eisenstein Z, editor. 4th International conference of numerical methods in geomechanics. Alberta: Edmonton; 1982. p. 1137–52.

[21] Barenblatt GI. Self-similarity: dimensional analysis, and intermediate asymptotics. J Appl Math Mech 1980;44:267–72.

[22] Hillerborg A, Modéer M, Petersson PE. Analysis of crack formation and crack growth in concrete by means of fracture mechanics and finite elements.Cem Concr Res 1976;6:773–81.

[23] Schmidt RA. A microcrack model and its significance to hydraulic fracturing and fracture toughness testing. In: Proc 21st US symp on rock mech; 1980. p. 581–90.

[24] Wittmann FH, Mihashi H, Nomura N. Size effect on fracture energy of concrete. Engng Fract Mech 1990;35:107–15.

[25] Erdogan F, Sih GC. On the crack extension in plates under plane loading and transverse shear. J Basic Engng, Trans ASME 1963;85:519–25.

[26] Williams ML. On the stress distribution at the base of a stationary crack. J Appl Mech 1957;24:109–14.

[27] ACI 318-08. Building code requirements for reinforced concrete. American Concrete Institute, Detroit; 2008.

[28] ACI 544.4R-88. Design considerations for steel fiber reinforced concrete (reapproved 2009). American Concrete Institute, Detroit; 2009.

[29] ACI-ASCE Committee 441. High strength concrete columns: state of the art. Am Concr Inst Struct J 1997;94(3):325–35.

[30] Aoude H, Cook WD, Mitchell D. Axial load response of columns constructed with fibres and self-consolidating concrete. ACI Struct J 2009;106(03):349–57.

[31] Bae S, Bayrak O. Seismic performance of reinforced concrete columns: P–D effect. ACI Special Publ 2006;236:61–80.

[32] Bai ZA, Au FTK. Ductility of symmetrically reinforced concrete columns. Mag Concr Res 2009;61(5):345–57.